Energy and Environment Focus
Vol. 7, pp. 1–9, 2022
www.aspbs.com/efocus

ARTICLE

Nitrogen Dioxide Gas Sensing Properties of Nanocrystalline In_2O_3 Thick Films for Environmental Protection

S. C. Kulkarni* and D. K. Halwar

The Sol–gel method was utilised to synthesise the nanocrystalline In_2O_3 powder with a cubic structure in the current study. Thick film samples of In_2O_3 powder were prepared on an alumina substrate. A low-cost and straightforward screen-printing method was used for making the film samples. The prepared samples were subjugated to firing at different temperatures in a range of 700 to 850 °C with 50 °C increment. This temperature range assured much better adhesion of films on the alumina substrate. The X-ray diffraction (XRD) study revealed the cubic phase along (222) orientation. The electrical characterization study confirmed the n-type semiconducting nature of the film samples. The film samples fired at 700 °C showed a relatively low resistivity compared to those fired at different temperatures. The particle size was found small with an enormous surface area. The morphology study using scanning electron microscopy (SEM) showed that the particle size also increased as the firing temperature was increased. Film samples fired at 700 °C were also exhibited higher sensitivity and selectivity for nitrogen dioxide gas of 100 ppm concentration at 100 °C operating temperature.

Keywords: Thick Film Sensors, Nanocrystalline, Gas Sensor, Screen Printing, Sensitivity.

1. INTRODUCTION

These days, everyone is aware of unnatural climate change, global warming, greenhouse effect etc., caused due to environmental pollution. The detection of NO_2 gas is significant in ecological insurance, which causes ozone depletion in the atmosphere, and its exposure would induce health disorders such as pulmonary edema and fatality [1]. Hence, there is an incredible enthusiasm for developing gas sensors that use oxides of metals as base semiconductors to detect NO_2. The metal oxide semiconductors such as WO_3 [2], In_2O_3 [3–6] and SnO_2 [7] can be effectively utilized for gases like NO_2 and O_3 that tend to oxidize. The interaction of these gases with n-type semiconductors induces higher resistance. Because of capturing of the electrons from semiconductor's conduction band, there is an increase in resistance, which is a surface process.

In_2O_3 is a notable conducting transparent oxide (TCO) with a wideband distance (3–4 eV) that assumes an additional standard role in various practical applications like an optoelectronic device, catalyst, dye-sensitized solar cells, including gas sensors. Lately, nano-sized homogeneous Indium Oxide grains have been created by chemical procedures like the Sol–gel method. The developed In_2O_3 film samples are crucial in the applications of gas sensing. Gurlo et al. [8] investigated thin films synthesized using the Sol–gel technique that exhibited an elevated response for NO_2 at 150 °C. Various reports demonstrated that thick and thin films primarily established on cubic In_2O_3 are fragile to small concentration of NO_2 and O_3 present in the air as opposed to the less sensitive carbon monoxide [9, 10]. In_2O_3 Sol–gel developed films of intermediate grain size ranging from 5 to 30 nm had shown the best response towards NO_2 gas. Therefore, for pragmatic applications, the development of Indium Oxide fine grains with crystal structure controlled grain size and shape is vital. Multiple technologies are utilized to develop In_2O_3 powder apt for thick films, but sol–gel is the most straightforward technique. The sensing layer's morphology assumes a vital role in the performance of a device, which is dependent on manufacturing practices and techniques. The Physical

Department of Electronic Science, M.S.G. Arts, Science and Commerce College, Malegaon, S.P.P.U, Pune, M.S. 423105, India
*Author to whom correspondence should be addressed.
Email:
Received:
Accepted:

Table I. Summary of literature survey.

Material	Synthesis method	NO_2 concentration (ppm)	Optimal temperature (°C)	Sensitivity/Response	References
In_2O_3	Sol–Gel and HVTE	0.7	250	10	[11]
In_2O_3 nano sheets	Hydrothermal	50	250	164	[12]
In_2O_3 nanoribbon	AC Electrophoretic	5	200	70	[13]
In_2O_3 nanowires	Hydrothermal	1	250	2.57	[14]
In_2O_3:SnO_2	RF Magnetron sputtering	250	250	7.5	[15]
In_2O_3:Gd_2O_3	Sol–gel	100	195	79	[16]
In_2O_3 microsphere	Solvent-thermal	5	250	1.5	[17]
In_2O_3:MoO_3,	Sol–gel	1	250	23	[12]
In_2O_3:Au	RF-sputtered	10	350	14.26	[19]
In_2O_3 (0.07)	Spray pyrolysis	100	150	33.45	[20]
In_2O_3:Zn Nanowire	Electro spinning	50	130	5	[21]

Vapour Deposition (PVD) and Chemical Vapour Deposition (CVD) are a few procedures employed for deposition of thin film. The Indium Oxide thick and thin films have been studied for gas sensing by many researchers by using various synthesis methods and nanostructures. Table I summarizes the literature survey.

A few reports are found on the study of the properties of screen-printed Indium oxide (In_2O_3) thick films as NO_2 gas sensors up to the present time. So, in the present study, nanocrystalline In_2O_3 powder was synthesised using simple Sol–gel technique, and the samples of thick films were prepared using a feasible and efficient screen-printing method. The alumina substrate was the ultimate choice for deposition of the thick film. The study of Indium oxide (In_2O_3) thick film's gas sensing properties was done with particular reference to the effect of firing temperature of these films on the gas sensing properties of NO_2.

2. EXPERIMENTAL DETAILS

2.1. Nanocrystalline In_2O_3 Powder Synthesis

The sol–gel method was used to synthesize nanocrystalline In_2O_3 powder. Indium nitrate solution was prepared at a concentration of 0.4 M using Indium (III) Nitrate hydrate (Sigma Aldrich, 99.99%, metal basis) and bi-distilled water. Until it became apparent, the solution was stirred. For the pH adjustment up to 9, while stirring, the solution of ammonia was inculcated dropwise. The precipitate was noticeable in no time. Stirring was carried out for an hour. However, the solution was centrifuged for 30 minutes at 5000 RPM to isolate the precipitation (REMIR–24). Then it was washed several times with bi-distilled water infused methanol to get rid of excessive ammonia ions. The distinctive white-coloured precipitate in the ambient air was sintered for an hour. The $In(OH)_3$ to Indium Oxide phase transformation occurred at the temperature of 400 °C. So, 400 °C was chosen as the calcination temperature, where complete removal of N-radicals occurs. The powder phase was corroborated with the help of XRD spectra. The Grain size was calculated with the help of Scherer's formula.

2.2. Sensor Fabrications

The In_2O_3 nanocrystalline laboratory synthesized yellowish powder was used for fabrication of thick film gas sensors. The paste for preparing the thick films comprised a solid and liquid phase ratio of 70:30 proportion. The solid phase consisted of a synthesized In_2O_3 powder and a glass frit, while the liquid phase was the temporary binder (organic medium). The calcinated Indium Oxide powder with 5 weight % of lead borosilicate glass frit acted as the functional material, while Ethyl Cellulose (EC, Aldrich), Butyl Carbitol Acetate (BCA, Aldrich) were utilised as interim binders. Due to binder, the paste acquires a significant thixotropic property. The mixture of EC and calcined powder of Indium Oxide was finely ground in mortar and pestle for 45 minutes. After that, a few drops of BCA were poured slowly into the ground powder and mixed thoroughly to achieve a paste with the desired viscosity [22]. The paste with the desired viscosity could easily pass via the screen pores and splash uniformly on the alumina substrate.

Later, the prepared paste was used for screen printing (140 mesh of nylon no.355) of the films on the alumina substrate (96% pure Kyocera). The film size selected was 20×10 mm^2. Figure 1 depicts the accurate dimensional extent of this device. Screen-printed thick film samples were then dried below the Infra-Red lamp (250 W, Philips) for half an hour to eliminate the organic vehicle. Then, the samples were fired at temperatures ranging from 700 °C to

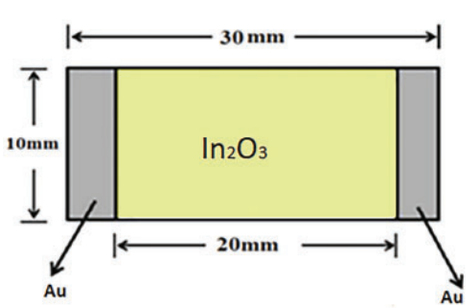

Fig. 1. Structure of In_2O_3 thick film sensor.

850 °C, increasing by 50 °C. The time of firing cycle and soaking was 45 minutes and 10–15 minutes, respectively. The electrical contacts were made to the developed films by depositing the silver coating on opposite ends. A profilometer (Dektek-150) was used to measure the thickness of the samples (Force subjected was 5 mg) and was found to be 16 μm (± 2 μm).

3. CHARACTERIZATION

3.1. Structural and Morphological Studies

The powder sample was subjected to Transmission Electron Microscopy (TEM). The TEM Model used was Philips CM-200) operating at 200 kV. The particle size, selected area diffraction pattern was studied. The film's morphological and elemental composition study was carried with the aid of Field Emission Electron Microscopy (FESEM). The model of FESM used was Zeiss Ultra 55 with Oxford EDAX system.

Further, the crystallinity and material phases of the calcined Indium oxide powder and the prepared film samples was studied using XRD (Make: Bruker D8, Advance) with Cu–Kα Radiation $\lambda = 1.542$ Å) from 20° to 80° Bragg's angle. The specific surface area of the film sample material was measured using the SMART SORB 90/91 apparatus. For this, the BET method was used.

3.2. Electrical Characterization

The study of the measurement of electrical resistance of thick films was carried by using the half bridge technique [23]. Figure 2 depicts the In_2O_3 thick film resistance variation with operating temperature for firing temperature range from 700 °C to 850 °C in the air atmosphere. The graph shows semiconductor behaviour. The surface characteristics such as grain size, surface area and crystallinity of the sample change due to firing temperature [24]. With an increase in the firing temperature of thick film samples, their electrical resistance decreased due to the entrapment of electrons or adsorbed low concentration oxygen on the surface. So, the increased grain size of the film material was a result of increased firing temperature.

3.3. Gas Sensing Characterizations

The ppm rate gas sensing features for fired films are determined under standard laboratory conditions employing the built-in single static measurement system. The samples for 100 ppm concentrations of NO_2 and H_2S gas and 500 ppm of NH_4 and C_2H_5OH are described. The properties of gas sensing have been tested based on the operating temperature.

The film sensor's temperature was increased in gradation of 10 °C from ambient temperature to 300 °C in the air and the test gas ambient (mixture of wind and test-gas). The corresponding electrical resistance readings were noted down at every incremental step of the operating temperature. The change in the electrical resistance of the film samples as a function of the temperature in both air and test-gas ambient was measured. The relative difference in the electrical resistance is the measure of the gas sensing behaviour of the film sample.

The sensitivity (S) of the film sample for oxidizing gases NO_2, H_2S, NH_3 and C_2H_5OH at various operating temperatures was determined by the formula,

$$S = \left| \frac{R_g - R_a}{R_a} \right| \quad (1)$$

Where R_a = film resistance in the air ambient and R_g = film resistance in test-gas plus air ambient, respectively, at the same operating temperature.

At the optimum temperature of certain test gas, its ppm concentration was varied, and the response of the film sample in the form of a change in its electrical resistance was noted down. From this information, a sensitivity curve was drawn for the sensor calibration.

4. RESULTS AND DISCUSSION

4.1. Structural and Morphological Studies

The TEM images of the calcined Indium oxide powder and its corresponding Selected Area Electron Diffraction (SAED) patterns have been demonstrated in Figure 3. The spherical shape is shown by most of the particles. The size of the particles varies from 20 to 30 nm.

The spotty ring pattern with no additional diffraction spot is seen in the SAED pattern of the In_2O_3 thick film sample. The presence of the rings in second phases of the SAED pattern confirms its crystalline cubic structure along (222) plane.

The X-ray diffraction (XRD) spectra of calcined In_2O_3 powder are shown in Figure 4. The XRD spectra attentively match with JCPDS card number 06-0416. Figure 5 demonstrates XRD spectra of In_2O_3 thick films fired at 700 °C, 750 °C, 800 °C and 850 °C. The diffraction spectra of Figures 4 and 5 nearly match with JCPDS card number

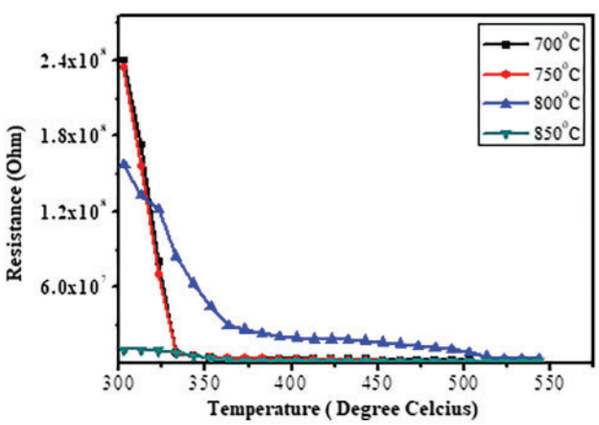

Fig. 2. Resistance variation alongside operating temperature for the In_2O_3 thick films. Firing temperatures from 700 °C to 850 °C.

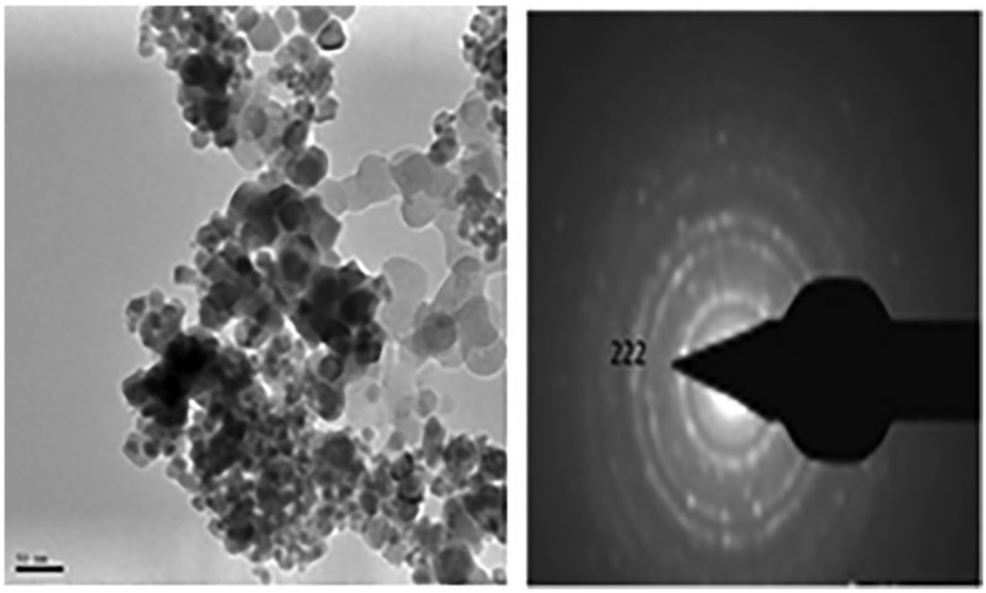

Fig. 3. TEM image and SAED pattern of In_2O_3 calcined nano powder.

06-0416. Due to the firing process of films, the intensity of diffraction peaks is found to increase. This increase in the intensity of diffraction peaks indicates greater crystallinity. The intensity of the peaks in the diffraction spectra of In_2O_3 thick films is found larger than that of the corresponding peaks of the diffraction spectra of calcined In_2O_3 powder. This might be due to the firing process undertaken for the thick films. The notable enlargement of the grain size with increased firing temperature conforms with the earlier reports [25]. Due to the alumina substrate, a few numbers of peaks of Al_2O_3 are observed [26].

From the XRD spectra, it is observed that the peaks along the (222) plane have a greater intensity. This indicates that the films have a preferred orientation along (222) plane. The size of the crystallite was computed with the aid of Scherer's formula [24] as,

$$D = \frac{0.9\lambda}{\beta \mathrm{Cos}\theta} \tag{2}$$

The sticking tape method was used to check the film's adhesiveness to the substrate. As shown in Figure 6, due to the agglomeration of particles results in enlarged grain size as the film's firing temperature is increased [27]. The FESEM images of In_2O_3 thick film sensors fired at 700 °C, 750 °C and 800 °C are shown in Figures 7(a)–(c). From FESEM images, it has been confirmed that the size of the particle has increased due to the increased firing temperature. The particle size of the film sample fired at 700 °C

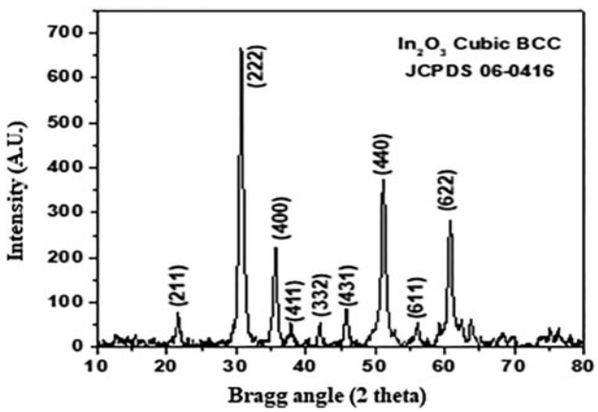

Fig. 4. XRD spectra of In_2O_3 nano powder.

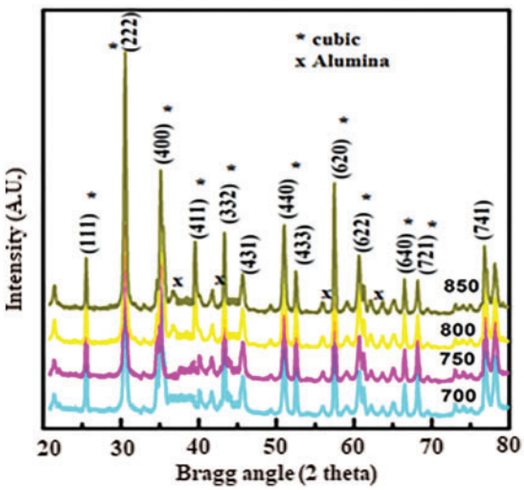

Fig. 5. XRD spectra of In_2O_3 thick films fired at 700 °C, 750 °C, 800 °C and 850 °C temperature.

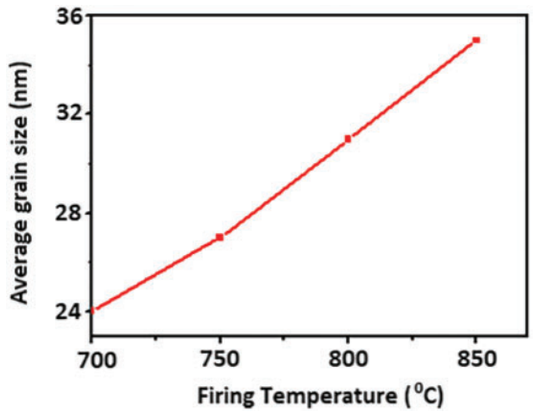

Fig. 6. Variation of average grain size with the firing temperature.

was determined to be the least (29 nm). The values of average particle size of film samples fired at 700 °C, 750 °C and 800 °C are shown in Table II. The EDAX analysis was utilised to confirm elemental composition of In_2O_3 thick films fired at 700 °C, 750 °C and 800 °C temperatures.

Table II. Specific surface area and particle size of In_2O_3 thick films fired at 700 °C, 750 °C and 800 °C.

Firing temperature (°C)	Surface area by BET technique (m^2/gm)	Average particle size from FESEM (nm)
700	39.8	29
750	32.9	35
800	29.87	42

The elemental composition of films is shown in Table III. The EDAX spectra of Figures 8(a)–(c) show the presence of only In (Indium) and O (oxygen). With the increase in firing temperature, there is a decrease in the mass percentage of oxygen due to the discharge of extra oxygen [28]. The non-stoichiometric nature of In_2O_3 films is confirmed from the EDAX spectra. For measuring the specific surface area, the deposited film material was battered and scratched from the alumina substrate and then using a BET method, the specific surface area was measured. The measured values of the specific surface area of In_2O_3 samples fired at 700 °C, 750 °C and 800 °C temperatures are shown in Table II.

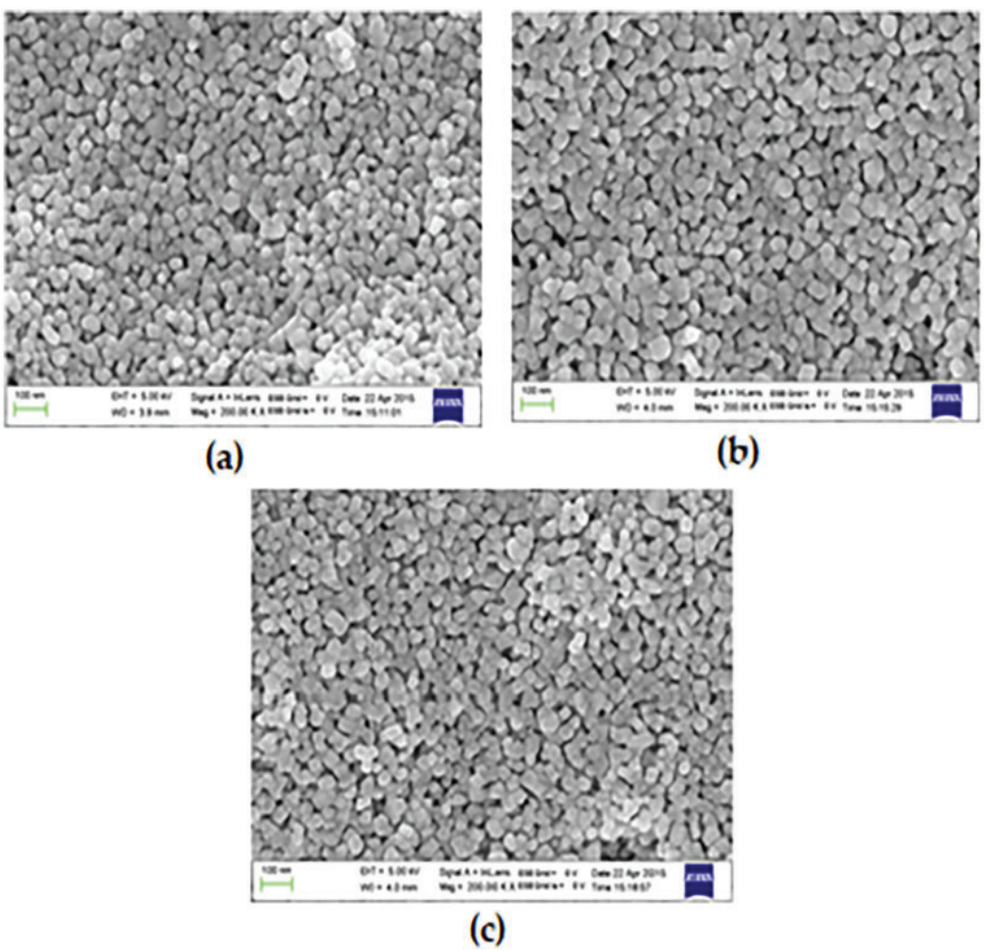

Fig. 7. FESEM images of In_2O_3 thick film sensors. Firing temperature (a) 700 °C (b) 750 °C (c) 800 °C.

Table III. Elemental composition of In_2O_3 thick films fired at 700 °C, 750 °C and 800 °C.

Firing temperature (°C)	Element	Mass%
700	In	74.87
	O	25.13
750	In	75.30
	O	24.70
800	In	79.15
	O	20.85

4.2. Firing Temperature Optimization

The factors like large surface area, small particle size, and better adhesion of the films to the alumina substrate help decide the optimum firing temperature of the film samples. The In_2O_3 samples fired at 700 °C are observed more adhesive to the alumina substrate than those fired at different temperatures. The sticking tape method was used to test the adhesion of the films. From FESEM images, it has been confirmed that the particle size of the film sample fired at 700 °C was determined to be the least (29 nm) and has a large surface area than that of the films fired at other temperatures. So, for gas sensing characterization, the temperature of 700 °C was considered as the optimum temperature.

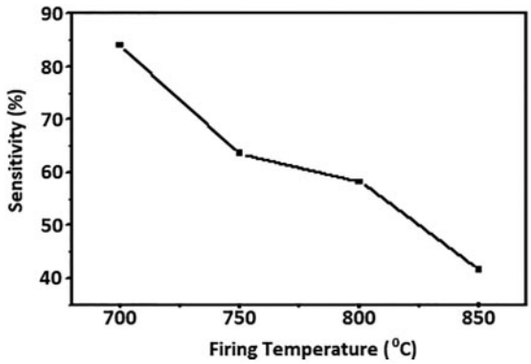

Fig. 9. Fluctuation of sensitivity alongside the firing temperature for 100 ppm NO_2 gas at 100 °C operating temperature.

4.3. Performance of Sensor

The study of gas sensing behaviour of In_2O_3 thick film samples was carried out for the NO_2 gas as a function of the operating temperature. Figure 9 demonstrates the fluctuation of sensitivity of the In_2O_3 thick film sensor alongside the firing temperature. The film sensors were tried for a 100 ppm concentration of NO_2 gas. It has been observed that the film samples fired at 700 °C exhibit the greatest sensitivity to the test-gas. Figure 10 demonstrates

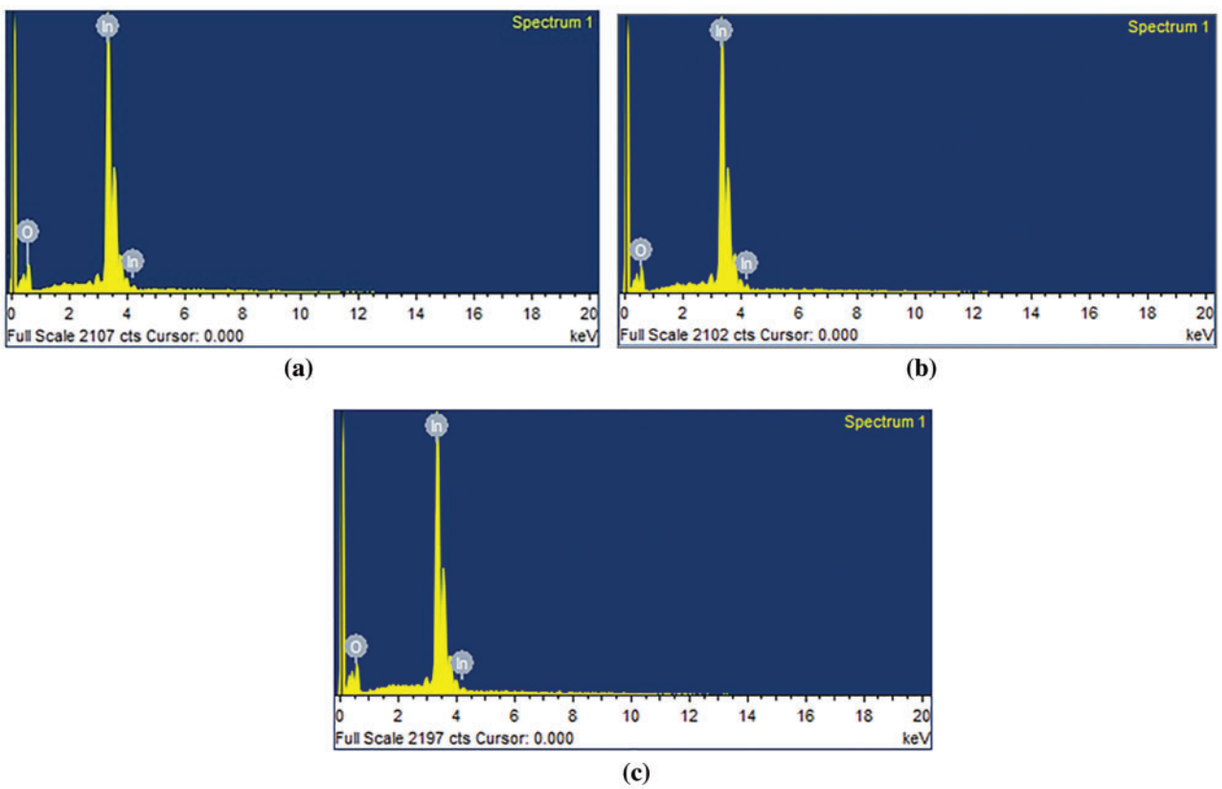

Fig. 8. EDAX spectra of In_2O_3 thick films. Firing temperature: (a) 700 °C (b) 750 °C (c) 800 °C.

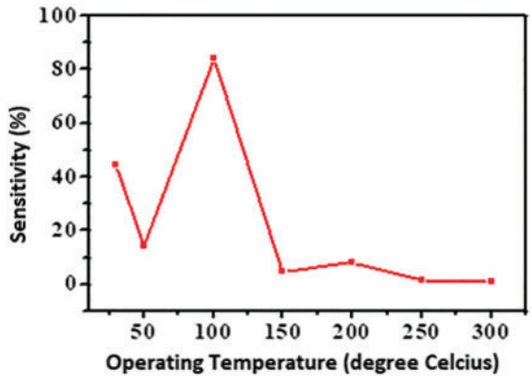

Fig. 10. Variation of sensitivity with operating temperature for 100 ppm concentration of NO_2 gas for In_2O_3 thick film sensor fired at 700 °C.

the variation of sensitivity in the film sensors at this firing temperature as a function of operating temperature.

The explanation of the NO_2 gas sensing mechanism is given in two ways by Eqs. (3)–(5). Equation (3) describes the adsorption of molecules onto the surface of the film either by extracting the electrons from the conduction band as per Eq. (3) or interaction with the chemisorbed oxygen on the surface according to Eqs. (4) and (5) [29].

$$NO_{2(gas)} + e^- \rightarrow NO^-_{2(ads)} \quad (3)$$

$$NO_{2(gas)} + O^-_{2(ads)} + 2e^- \rightarrow NO^-_{2(ads)} + 2O^-_{(ads)} \quad (4)$$

$$NO_{2(gas)} + O^-_{(ads)} \rightarrow NO^+{}_{(ads)} + 2O^-_{(ads)} \quad (5)$$

The above equations show that the electrons are depleted in the reactions. This causes increased resistance in the film throughout the exposure. It is observed that sensitivity increases or decreases due to the adsorption and desorption phenomenon [30]. The highest sensitivity factor is due to the smallest grain size within the film, as seen in FESEM. Selectivity is of the utmost importance in instances where gas sensors are involved. Figure 11 demonstrates the selectivity of film samples for reducing gases ammonia (NH_4), ethanol (C_2H_5OH), hydrogen sulphide (H_2S) and NO_2 at 100 °C operating temperature.

It is evident from Figure 11 that the film's sensitivity to NO_2 gas is considerable and offers a pretty good selectivity to it against the other gases. The sensitivity of In_2O_3 thick film samples to NH_4, C_2H_5OH and H_2S gases at 100 °C operating temperature is shown in the inset of Figure 11 separately due to its lower value compared to the value of sensitivity NO_2 gas. One of the crucial specifications of the thick film gas sensor is the calibration curve. The calibration curve is the graph of sensor sensitivity against the ppm gas concentration. Figure 12 shows the variation of the sensor's sensitivity with ppm concentration of NO_2 gas at 100 °C. The sensitivity is found to increase with NO_2 gas ppm concentration.

The time required for the film sensor to attain 90% of its maximum sensitivity following the injection of target gas in the chamber is the response time and the time required to reduce to its 10% of maximum sensitivity value just after the turn off of the gas is referred to as its recovery time.

The response time of In_2O_3 film sensor for 100 ppm concentration NO_2 gas has been noted as 20 seconds and the recovery time is relatively more of the adsorption process occurred according to the following Eq. (6). Figure 13 shows the recovery time and response time of the In_2O_3 thick film sensor to NO_2 gas of 100 ppm concentration.

$$NO_{2(gas)} + \left(In^{2+}\right) \longleftrightarrow \left(In^{3+} + O^-\right) + NO_{(gas)} \quad (6)$$

Because of the adsorption process that occurs, the resistance of the film sensor increases.

A longer recovery time is observed due to the removal of chemisorbed oxygen. It confines the desorption of NO_2 gas on the sensor's surface, leading towards a significant recovery time [3] of 20 minutes.

$$2\left(In^{3+} + O^-\right) \longleftrightarrow 2\left(In^{2+}\right) + O_{2(gas)} \quad (7)$$

It has been observed that the resistance of the film sensor is relatively higher at 100 °C operating temperature.

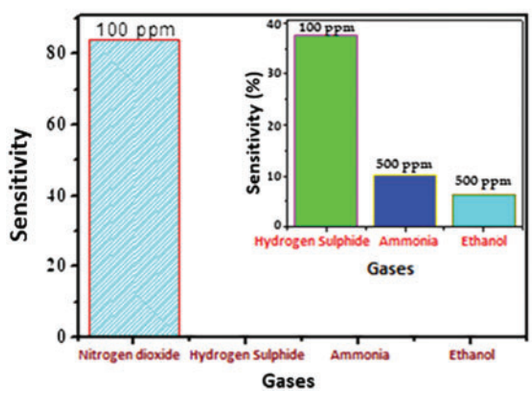

Fig. 11. Selectivity of In_2O_3 thick film samples for NH_4, C_2H_5OH, H_2S and NO_2 gases at 100 °C operating temperature.

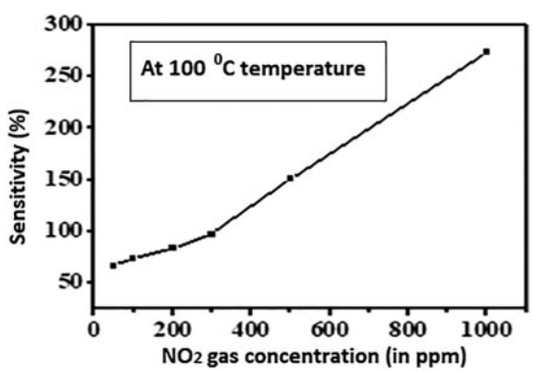

Fig. 12. Sensitivity of In_2O_3 thick films as function of NO_2 gas concentration (in ppm) at 100 °C operating temperature.

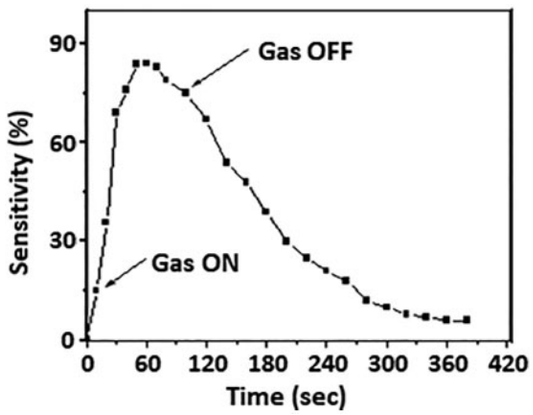

Fig. 13. Recovery time and response time of the In_2O_3 thick film sensor for 100 ppm concentration NO_2 gas.

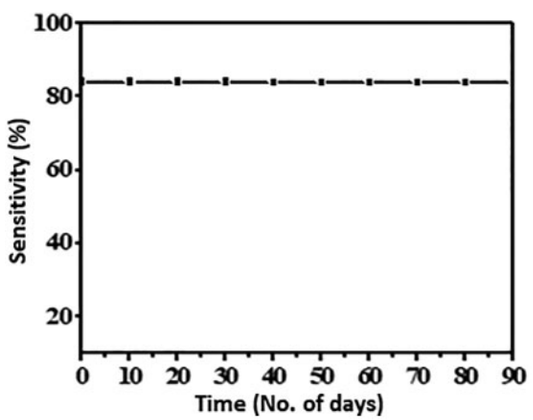

Fig. 14. Sensing stability of undoped In_2O_3 thick film sensor of 100 ppm concentration NO_2 gas.

The rate of desorption is proportional to the sensor's operating temperature, and if the operating temperature is further increased, it becomes comparable to the rate of adsorption. This results in lower sensitivity and faster recovery [3]. For testing the stability of a sensor, the measurements were repeated for three months for a 100 ppm concentration of NO_2 gas and no remarkable variations were noted in the readings. This confirmed the excellent stability of the film sensor during the test period. The noted results are shown in Figure 14.

5. CONCLUSIONS

The In_2O_3 thick film sensors were processed with a simple and modular screen printing technique with optimized 5% glass frit. The glass frit was used as a permanent binder. The XRD analysis showed that In_2O_3 thick films fired at 700 °C to 850 °C exhibit the cubic BCC structure with preferred orientation along (222) plane. The crystallite size enlarges upon increasing the firing temperature of the thick films. The film samples fired at the temperature of 700 °C exhibit a high sensitivity towards NO_2 gas at 100 °C. BET measurement showed a large specific surface area for the film samples, which were fired at 700 °C. It is found that the film sensor shows a good selectivity towards NO_2 gas against reducing gases like hydrogen sulphide, ethanol and ammonia at 100 °C temperature. The sensor's sensitivity has been found proportional to the ppm concentration of NO_2 gas. The response time of ~20 seconds and a recovery time of ~20 minutes have been recorded. Excellent reproducibility and stability have been exhibited by the sensor fabricated in our laboratory.

Acknowledgments: One of the authors (SCK) acknowledges the University Grants Commission, New Delhi, for the teacher fellowship award under the XII plan. The authors are grateful to 'MG. Vidyamandir's management for their patronage to carry out this work.

References and Notes

1. Storke, T.K.H., Coles, G.S.V. and Ferkel, H., **2002**. High sensitivity NO_2 sensors for environmental monitoring produced using laser ablated nanocrystalline metal oxides. *Sensors and Actuators*, *B85*, pp.239–245.
2. Zeng, J., Hu, M., Wang, W., Chen, H. and QinV, Y., **2012**. NO_2-sensing properties of porous WO_3 gas sensors based on anodized sputtered tungsten thin films. *Sensors and Actuators*, *B161*, pp.447–452.
3. Gurlo, A., Barsan, N., Ivanovskaya, M., Weimar, U. and Gopel, W., **1998**. In_2O_3 and MoO_3–In_2O_3 thin film semiconductor sensors: Interaction with NO_2 and O_3. *Sensors and Actuators*, *B4*, pp.92–99.
4. Sowti Khiabania, P., Marzbanrada, E., Zamani, C., Riahifar, R. and Raissi, B., **2012**. Fabrication of In_2O_3 based NO_2 gas sensor through AC electrophoretic deposition. *Sensors and Actuators*, *B166–167* pp.128–134.
5. Xiaolong, H., Liyuan, T., Hongbin, S., Biao, W., Yuan, G., Peng, S., Fengmin, L., Geyu, L., **2015**. Highly enhanced NO_2 sensing performance of Cu-doped In_2O_3 hierarchical flowers. *Sensors and Actuators*, *B221*, pp.297–304.
6. Zhang, D., Liu, Z., Li, C., Tang, T., Liu, X., Han, S., Lei, B. and Zhou, C., **2004**. Detectation of NO_2 down to ppb levels using individual and multiple In_2O_3 nanowire devices. *Nano Letters*, *4*(10), pp.1919–1924.
7. Sharma, A., Tomar, M. and Gupta, V., **2011**. SNO_2 thin film sensor with enhanced response for NO_2 gas at lower temperatures. *Sensors and Actuators*, *B156*, pp.741–752.
8. Gurlo, A., Ivanovskaya, M., Pfau, A. and Weimar, U., **1997**. Sol–gel prepared In_2O_3 thin films. *Thin Solid Films*, *307*(1–2), pp.288–293.
9. Ivanovskaya, M., Gurlo, A. and Bogdanov, P., **2001**. Mechnism of O_3 and NO_2 detectation and selectivity of In_2O_3 sensor. *Sensors and Actuators*, *B77*(1–2), pp.264–267.
10. Chung, W.Y., **2001**. Gas-sensing properties of spin coated indium oxide film on various substrate. *Journal of Materials Science: Materials Electron*, *12*, pp.591–595.
11. Cantalini, C., Wlodarski, W., Sun, H.T. and Atashbar, M.Z., **2000**. NO_2 response of In_2O_3 thin films Gas sensors prepared by sol–gel and vacuum thermal evaporation techniques. *Sensors and Actuators*, *B65*, pp.101–104.
12. Gao, L., Cheng, Z., Xiang, Q., Zhang, Y. and Xu, J., **2015**. Porous corundum type In_2O_3 nanosheets: Synthesis

and NO_2 sensing properties. *Sensors and Actuators*, *B208*, pp.36–443.

13. Khiabani, P.S., Marzbanrad, E., Zamani, C., Riahifar, R. and Raissi, B., **2012**. Fabrication of In_2O_3 based NO_2 gas sensor through AC-electrophoretic deposition. *Sensors and Actuators*, *B166–167*, pp.128–134.

14. Xu, P., Cheng, Z., Pan, Q., Xu, J., Xiang, Q., Yu, W. and Chu, Y., **2008**. High aspect ratio In_2O_3 nanowires: Synthesis, mechanism and NO_2 gas-sensing properties. *Sensors and Actuators, B: Chemical*, *130*(2), pp.802–808.

15. Sberveglieri, G., Groppelli, S. and Coccoli, G., **1988**. Radio frequency magnetron sputtering growth and characterization of indium tin (ITO) thin films for NO_2 gas sensors. *Sensors and Actuators*, *15*(3), pp.235–242.

16. Niu, X., Zhong, H., Wang, X. and Jiang, K., **2006**. Sensing properties of rare earth oxide doped In_2O_3 by Sol–gel method. *Sensors and Actuators*, *B115*(1), pp.234–238.

17. Cheng, Z., Song, L., Ren, X., Zheng, Q. and Xu, J., **2013**. Novel lotus root slice-like self-assembled In_2O_3 microspheres: Synthesis and NO_2-sensing properties. *Sensors and Actuators*, *B176*, pp.258–263.

18. Barsan, N., Ivanovskaya, M., Weimar, U. and Göpel, W., **1988**. In_2O_3 and MoO_3–In_2O_3 thin film semiconductor sensors: Interaction with NO_2 and O_3. *Sensors and Actuators*, *B47*(1–3), pp.92–99.

19. Steffes, H., Imawan, C., Solzbacher, F. and Obermeier, E., **2001**. Enhancement of NO_2 sensing properties of In_2O_3-based thin films using an Au or Ti surface modification. *Sensors and Actuators*, *B78*(1–3), pp.106–112.

20. Patil, S.P., Patil, V.L., Shendge, S.S., Harale, N.S, Vana, S.A., Kim, J.H. and Patil, P.S., **2016**. Spray pyrolyzed indium oxide thick films as NO_2 gas sensor. *Ceramics International*, pp.1–9.

21. Ueda, T., Boehme, I., Hyodo, T., Shimizu, Y., Weimar, U. and Barsan, N., **2020**. Enhanced NO_2 sensing properties of Au loaded porous In_2O_3 gas sensor at low operating temperatures. *Chemosensors*, pp.1–14.

22. Kulkarni, S.C., Aher, C.S., Borse, R.Y., Bharate, B.G., AlDeyab, S.S., Ansari, S.G., and Khanna, P.K., **2012**. Gas sensing properties of nanocrystalline indium oxide synthesized by Sol–Gel method. *Advanced Science Letters*, *5*, pp.109–113.

23. Patil, A., Dighavkar, C., Borse, R., Patil, S. and Khadayate, R., **2012**. effect of Cr_2O_3 by doping and dipping on gas sensing characteristics of ZnO thick films. *Journal of Electron Devices*, *15*, pp.1274–1281.

24. Ryu, H.W., Park, B.S., Akbar, S.A., Lee, W.S., Hong, K.J., Seo, Y.J., Shin, D.C. and Park, J.S., **2003**. ZnO Sol-del derived porous film dor COI gas sensing. *Sensors and Actuators, B: Chemical*, *96*(3), pp.717–722.

25. Kulkarni, S.C. and Borse, R.Y., **2011**. Study on gas sensing performance of In_2O_3 thick film resistors prepared by screen printing technique. *Sensors & Transducers*, *125*(2), pp.194–204.

26. Kulkarni, S.C. and Patil, D.S., **2015**. Effect of $PdCl_2$ molarity on the gas sensing properties of nanocrystalline indium oxide. *Sensor Letters*, *13*(4), pp.294–299.

27. Garje, A.D. and Aiyer, R.C., **2007**. Effect of firing temperature on electrical and gas sensing properties of nano-SNO_2 based thick-film resistors. *International Journal of Applied Ceramic Technology*, *4*(5), pp.446–452.

28. Kiriakidis, G., Suchea, M., Christoulakis, S. and Katsarakis, N., **2005**. High performance gas sensing materials based on nanostructed metal oxide films. *Reviews on Advanced Materials Science*, *10*(3), pp.215–223.

29. Sonker, R.K., Yadav, B.C., Gupta, V. and Tomar, M., **2020**. Synthesis of CdS nanoparticle by Sol–gel method as low temperature NO_2 sensor. *Materials Chemistry and Physics*, *239*, p.121975.

30. Ansari, S.G., Boroojerdian, P., Sainkar, S.R., Karekar, R.N., Aiyer, R.C. and Kulkarni, S.K., **1996**. Effect of thickness on H2 gas sensitivity of SNO_2 nanoparticles based thick film resistors. *Journal of Materials Science: Materials Electron*, *7*, pp.267–270.